International Journal of Scientific Research and Management (IJSRM)
||Volume||07||Issue||12||Pages||MS-2019-01-07||2019||
Website: www.ijsrm.in ISSN (e): 2321-3418
DOI: 10.18535/ijsrm/v7i12.ms01

Effects of Sintering Temperature on Crystallinity, Morphology, and Photocatalytic Activity of Bi_2O_3

Mukholit, Heri Sutanto*, Ngurah Ayu Ketut Umiati, Eko Hidayanto

Department of Physics, Diponegoro University, Semarang Indonesia

Abstract
Bi_2O_3 has successfully been synthesized using precipitation method with sintering temperature variations of 400°C, 450° C, 500° C, 550° C, and 600° C. Crystallinity property of resulting Bi_2O_3 powder has also been tested with XRD and morphology properties were tested with SEM. Meanwhile, photocatalytic properties were tested by using it to degrade Rhodamine B under sunlight. Results of XRD tests show that differences in sintering temperature affect crystallite size. Increases in sintering temperature between 400° C and 500° C result in greater crystallite size, whereas sintering temperature between 550° C and 600°C result in smaller crystallite size. Results of SEM tests show that resulting Bi_2O_3 has rod-like structure, While results of degradation tests show that increases in sintering temperature enhances photocatalytic activities of Bi_2O_3, as evident with Bi_2O_3 undergoing sintering at 600°C was able to degrade Rhodamine B with 56.74% effectiveness and degradation rate of 0.007 ppm/min.

Keywords: Bismuth Oxide, Photocatalytic, Microstructure, Degradation, Sintering

Introduction

Over the past few years, research on semiconductor-based photocatalysis has been gaining interest as it has wide-ranging applications, from gas sensor, electrochromic material, solar energy conversion, optoelectronic devices, to optical layers [1][2][3]. Traditional photocatalytic materials such as TiO_2, ZnO, and $BiPO_4$ have incredible photocatalytic performance under ultraviolet light irradiation but their energy gaps are too wide to be able to absorb visible light [3][4][5]. This is quite a drawback as UV only makes up 5 % of the total sunlight reaching the Earth [6][7].Therefore, researchers try to develop photocatalytic materials that can be activated by visible light such as Bi_2O_3 with an energy gap of 2.8 eV[8][9][10].

Bi_2O_3 possesses advantageous characteristics such as significant photoluminescence, high reflective index (2.3), high photoconductivity, high thermal chemistry stability, low resistivity, being non-poisonous, and good photocatalytic activities [11][12][13]. Bi_2O_3 comes in six phases of: α-Bi2O3 (monoclinic), β-Bi_2O_3 (tetragonal), γ-Bi_2O_3 (body-centered cubic), δ-Bi_2O_3 (face-centered cubic), ε-Bi_2O_3 (orthorhombic), and ω-Bi_2O_3 (triclinic) [14]. Out of those six phases, α- Bi_2O_3 is the most stable, while β-Bi_2O_3 is slightly less stable than α-Bi_2O_3. Meanwhile, γ-Bi_2O_3, δ-Bi_2O_3, ε-Bi_2O_3 ω-Bi_2O_3 are metastable phases [15].

Methodology

Bi_2O_3 was synthesized using precipitation method as depicted in Figure 1. $Bi(NO_3)_3.5H_2O$ was used as Bi, HNO_3 source that served as solvent, and NaOH served as the catalyst. First, 0.5 g of $Bi(NO_3)_3.5H_2O$ was dissolved in 50 ml of 5%HNO_3 solution. The process was performed by stirring both materials using a stirrer. Afterwards, 250 ml of NaOH was added to the solution and was then further stirred using a stirrer for 2 hours in order to produce precipitate. Precipitate and solution were separated using filter paper before being heated to 120° C to evaporate the water and produce Bi_2O_3 powder. The Bi_2O_3 powder that no longer contain water was then undergoing sintering in a furnace at temperatures of 400°C, 450°C, 500°C, 550°C, and 600°C for 4 hours, respectively. Resulting materials were then designated samples A, B, C, D, and E. The next step was characterization. Characterizations were performed using XRD to find out their crystallinity and SEM-EDX to figure out their morphology.

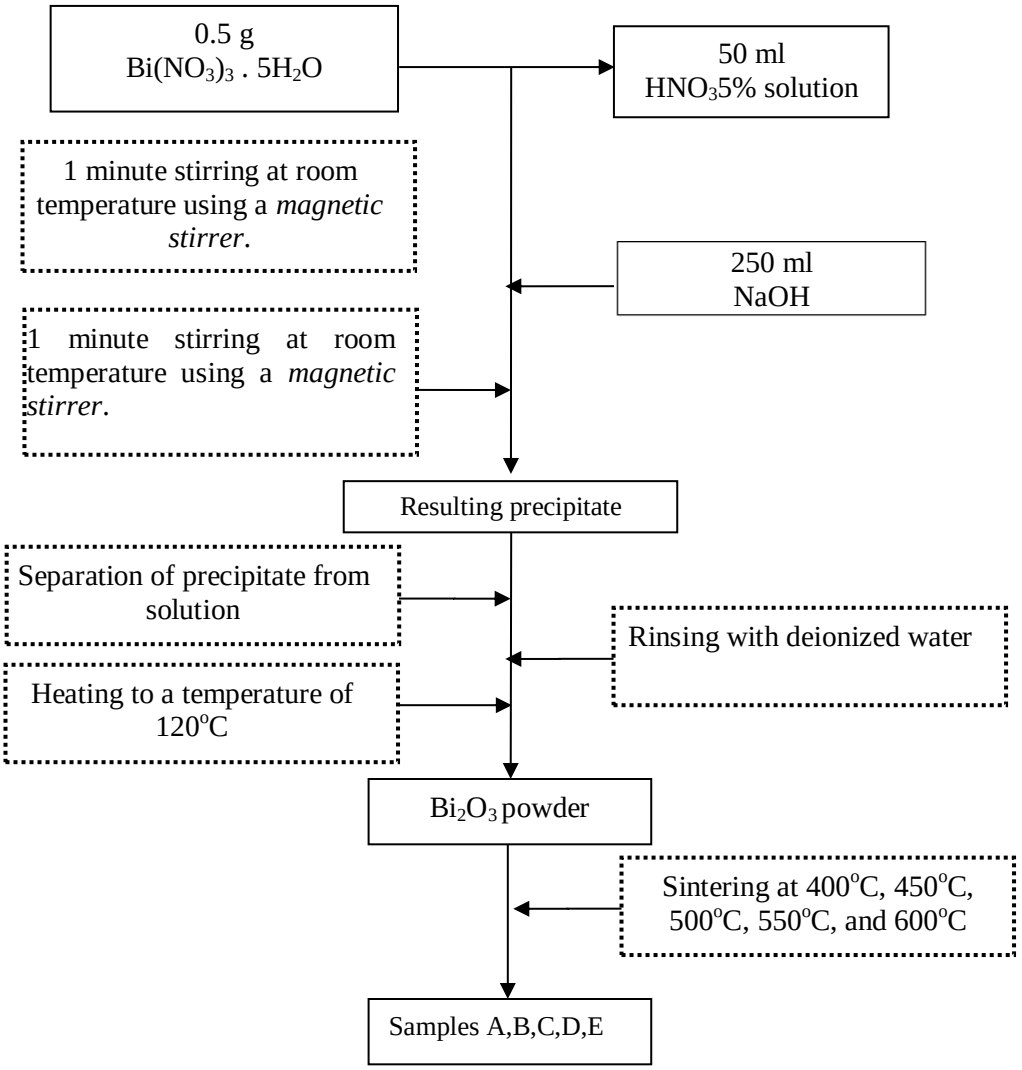

Figure 1. Bi_2O_3 synthesis using precipitation method

Results and discussion

XRD Analysis

Results of XRD analysis are depicted in Figure 2. Based on JCPDS, No. 27–0053, diffraction peaks are at 21.75°, 25.76°, 25.56°, 26.91°, 27.39°, 28.01°, 33.96°, 35.04°, 37.57°, 46.29°, 48.59°, 52.09°, 52.38°, 52.98°, 54.80°, 55.45°, 55.88°, 57.78°, 58.29°, 62.31°, 63.55°, which show diffraction of (020), (021), (002), (112), (121), (012), (202), (212), (113), (223), (104), (313), (322), (233), (241), (224), (323), (304), (143), (152), (213). In general, increasing sintering temperatures result in higher and sharper diffraction peaks. No diffraction peak was found in sample A. This means that sample A is amorphous. Sample B has three diffraction peaks. This means that 450^0 C is adequate to change amorphous structure into crystalline structure. Figure 2 also reveals that the number of diffraction peaks increases, as sintering temperature rises. This means that raising sintering temperatures speeds up transformation from amorphous Bi_2O_3 into crystalline Bi_2O_3. Higher sintering temperature results in better crystallite quality. This is supported by results from degradation test. Higher sintering temperature results in better degradation outcome. Higher crystallinity results in higher photocatalytic activities. Therefore, sample A is amorphous Bi_2O_3 with the lowest photocatalytic activity. In amorphous materials, electrons and holes play the role of easily recombined photocatalysis [16] Results from XRD test also reveal that crystallite size is affected by sintering temperature. Crystallite size is measured using the Scherrer formula (Equation 1) [17].

$$Cs = \frac{c\,\lambda}{FWHM\ (\cos\theta)} \quad (1)$$

With Cs is crystallite size, c is a constant (shape factor), λ is the X-Ray wavelength, FWHM is the full width at half maximum of characteristic diffraction peaks. Calculation results using Equation 1 are shown in Table 1.

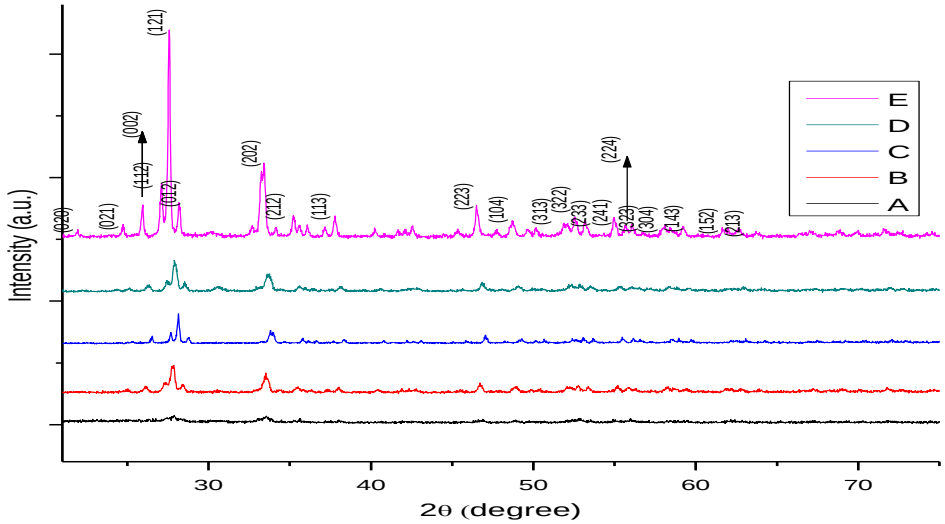

Figure 2. Results of XRD analysis

Table 1 Crystallite size

Sample	FWHM (rad)	2 theta (degree)	λ (nm)	D (nm)
A	-	-	-	-
B	0.322	27.573	0.154	25.437
C	0.287	27.794	0.154	28.544
D	0.159	27.927	0.154	51.458
E	0.147	28.141	0.154	55.658

It can be seen in Table 1 that FWHM decreases from sample A to sample E. This decrease in FWHM also confirms that crystallinity increases with rising sintering temperature. Table 1 also reveals that higher sintering temperature results in shifting diffraction peaks. Raising sintering temperature also affects crystallite size. Higher sintering temperature results in greater crystallite size.

SEM-EDX analysis

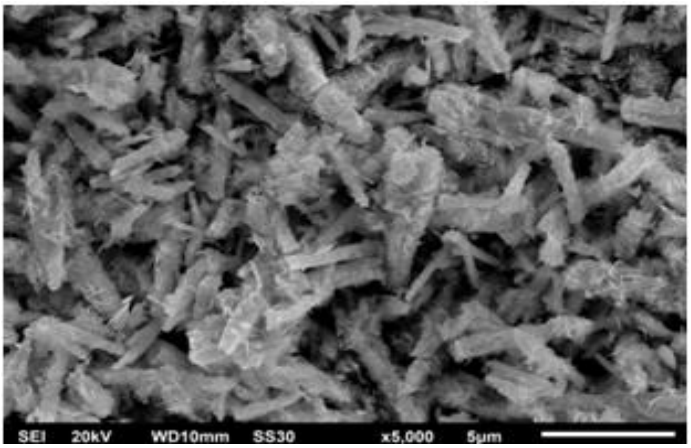

(A)

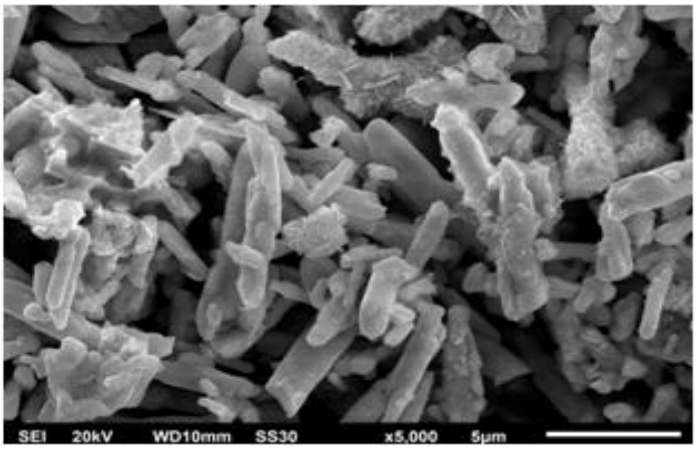

(B)

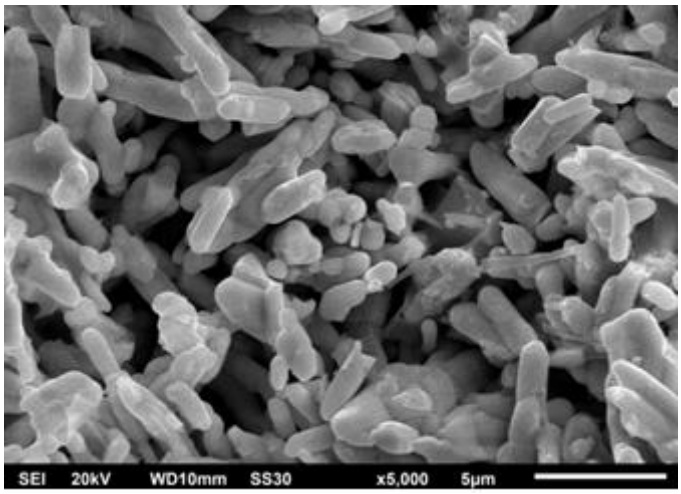

(C)

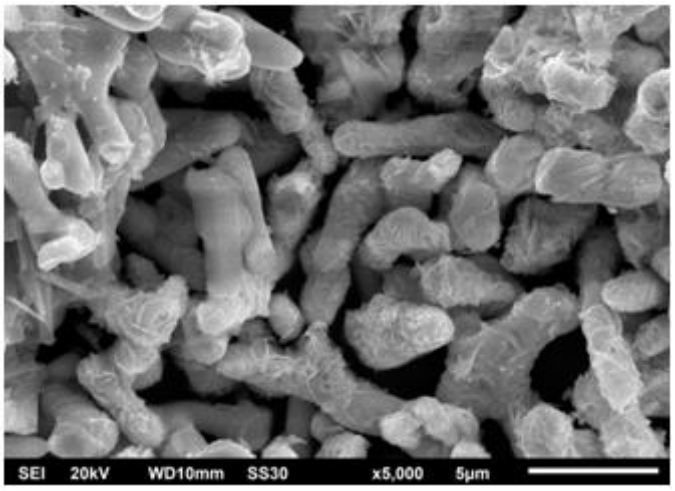

(D)

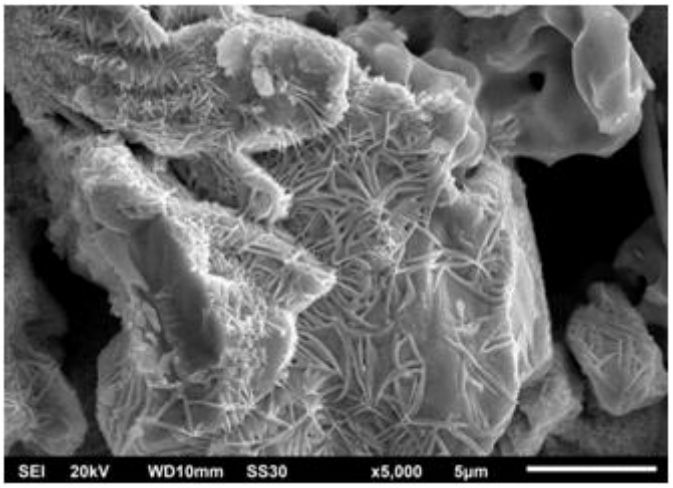

(E)

Figure 3. Results of SEM analysis

Results of SEM test show that sintering temperature affects Bi_2O_3 morphology. Figure 3. Shows that resulting Bi_2O_3 has rod-like structure. Sample A, which as sintered at 400° C, appears to have rough rod structure. Raising sintering temperature from 400°C to 500°C caused alteration in Bi_2O_3 rod structure, from being rough to become smoother. When sintering temperature was raised to 550°C, Bi_2O_3 particles started to experience agglomeration. Sintering at 600°C caused extensive agglomeration and the rod-like structure of Bi_2O_3 is no longer visible. SEM images also show that raising sintering temperature from 400°C to 500°C caused particle growth, whereas raising sintering temperature from 500°C to 600°C caused agglomeration. This means that the optimum temperature for particle growth is 500°C.

Degradation Test

Photocatalytic activity of Bi_2O_3 was tested for its ability to degrade 10 PPM of Rhodamine B (RhB). Rh B was chosen because it is an organic colorant that is widely used, despite the fact that it is not environmentally friendly [18]. An amount of 0.06 g of Bi_2O_3 photocatalytic powder was used to degrade 40 ml or Rh B. Degradation test has shown the success of reducing Rh B concentration as depicted in Figure 4.

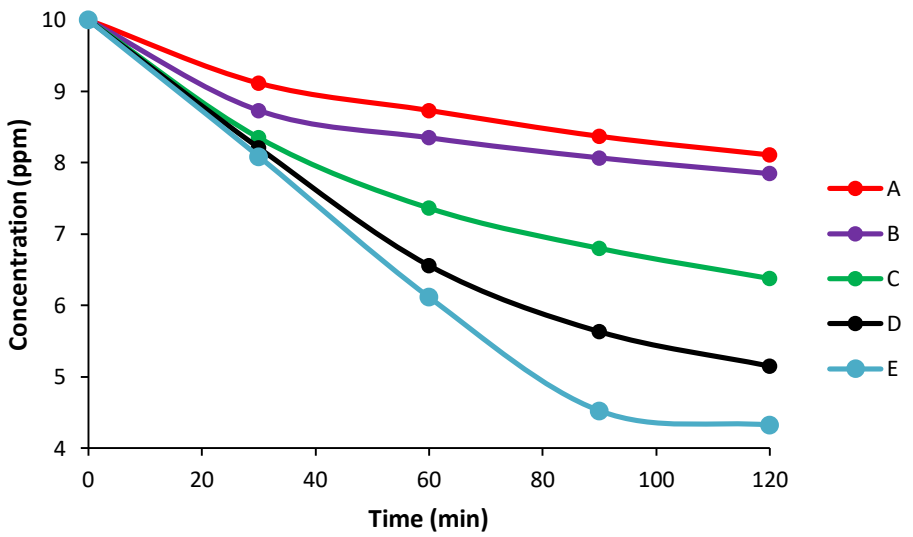

Figure 4. Lowering Rh B concentration every 10 minutes.

Results of degradation test show that sintering duration affects photocatalytic activity of Bi_2O_3, in which longer sintering period results in better photocatalytic activity. Therefore, final Rh B concentration with degradation using sample A is greatest, followed by those using samples B, C, D, and E. Figure 5. Figure 5 shows that sample E processes the highest photocatalytic activity of 56.74%, followed by samples D, C, B, and A, with photocatalytic activities of 48.49%, 36.22%, 21.53%, and 18.91%, respectively. In the meantime, Figure 6 reveals that sample E is capable of degrading Rn B the fastest, at a rate of 0.007 ppm/min, followed by samples D, C, B, and A, with degradation rates of 0.005 ppm/min, 0.003 ppm/min, 0.001 ppm/min and 0.001 ppm/min, respectively. This means that increasing sintering temperatures has successfully improved photocatalytic activity of Bi_2O_3. Improved photocatalytic activity relates to better crystallinity, as proven by XRD test results depicted in Figure 2. Hence, it can be concluded that crystallinity affects photocatalytic activity of Bi_2O_3. Meanwhile, morphology and crystallite size do not significantly affect photocatalytic activity.

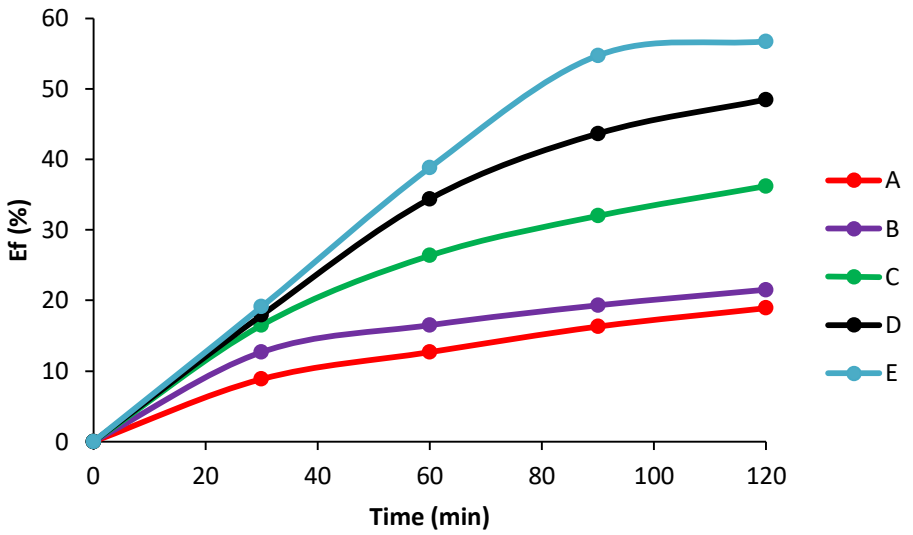

Figure 5. Photocatalytic effectiveness of Bi_2O_3 with varied sintering duration

Conclusion

This research found that different sintering temperatures affect crystallinity, morphology, and photocatalytic activity of Bi_2O_3. Crystallite size of Bi_2O_3 is optimum at sintering temperature of 500°C; with raising sintering temperature from 400° C to 500° C increases crystallite size. Raising sintering temperature from 500°C to 600°C decreases crystallite size. Therefore, the optimum crystallite size is reached at a temperature of 500°C. Raising sintering temperature from 400°C to 500°C increases crystallite size, and decreases band gap energy. In

the meantime, raising sintering temperature from 500°C to 600°C results in agglomeration. Results of degradation test found that photocatalytic activity is in line with sintering temperature. This means that higher sintering temperature results in higher photocatalytic activity.

Acknowledgements
Authors would like to acknowledge all member of Smart Materials Research Center (SMARC) Diponegoro University for supporting this research.

References

[1] Chia, W-K., Yang, C-F., Chen, Y-C., The effect of Bi_2O_3 compensation during thermal treatment on the crystalline and electrical characteristics of bismuth titanate thin films, International Volume, March 2008, Pages 379-384.
[2] Zhu, B.L., Zhao, X.Z., Study on structure and optical properties of Bi_2O_3thin films prepared by reactive pulsed laser deposition, Materials Volume, November 2006, Pages 192-198.
[3] Kalnaowakul, Phairatana, T., Ubolchollakhet, K., Sangchay, W., Rodchanarowan, A., Synthesis of Bi2O3-doped and TiO2-doped porous Lava for photocatalytic studies, Materials Today: Proceedings 5 (2018) 9312–9318.
[4] Wang, L., Zhang, J., Li, C., Zhu, H., Wenwen, Wang, W., Wang, T., Synthesis, Characterization and Photocatalytic Activity of TiO_2 Film/Bi_2O_3 Microgrid Heterojunction, Technology Volume, January 2011, Pages 59-63.
[5] Lim, H., Rawal, S.B., Integrated Bi_2O_3 nanostructure modified with Au nanoparticles for enhanced photocatalytic activity under visible light irradiation, Science: International Volume, June 2017, Pages 289-296.
[6] Hao, Q., Wang, R., Lu, H., Xie, C., Ao, W., Chen, D., Ma, C., Yao, W., Zhu, Y., One-pot synthesis of C/Bi/Bi2O3 composite with enhanced photocatalytic activity, Applied Catalysis B: Environmental 219 (2017) 63–72.
[7] Sutanto, H., Hidayanto, E., Mukholit, Wibowo, S., Nurhasanah, I., Hadiyanto, The Physical and Photocatalytic Properties of N-doped TiO_2 Polycrystalline Synthesized by a Single Step Sonochemical Method at Room Temperature, *Materials Science Forum, Vol. 890, pp 121-126.*
[8] D'Angelo, D., Fillice, Scarangella A, Iannazzo, Comagnini, Scallese, Bi_2O_3/Nexar® polymer nanocomposite membranes for azo dyes removal by UV–vis or visible light irradiation, Today Available online 15 December 2017.
[9] Zhang, L., Hoshimoto, Y., Taishi, T., Nakamura, I., Ni, Q., Fabrication of flower-shaped Bi_2O_3 superstructure by a facile template-free process,
[10] Guishui, L., Lijun, C., Bing, Z., Yi, L., 2016, Novel Bi_2O_3 loaded sepiolite photocatalyst: Preparation and characterization, Materials Letters 168 (2016) 143–145.
[11] Matysiak, W., Tański, T., Jarka, P., Nowak, M., Kępińska, M., Szperlich, P., Comparison of optical properties of PAN/TiO_2, PAN/Bi_2O_3, and PAN/SbSI nanofibers, Materials Volume, September 2018, Pages 145-151.
[12] Patil, S. P., Bethi, B., Sonawane, G. H., Shrivasta, V. S., Sonawane, S., 2015, Efficient adsorption and photocatalytic degradation of Rhodamine Bdye over Bi2O3-bentonite nanocomposites: A kinetic study, Journal of Industrial and Engineering Chemistry 34 (2016) 356–363.
[13] Gao., N., Lu, Z., Zhao, X., Zhu, Z., Wang, Y., Wang, D., Hua, Z., Li, C., Huo, P., Song, M., 2016, Enhanced photocatalytic activity of a double conductive C/Fe3O4/Bi2O3 composite photocatalyst based on biomass, Chemical Engineering Journal 304 (2016) 351–361.
[14] Guan, Z., Wang, H., Wang, X., Hu, J., Du, R., 2018, Title: Fabrication of heterostructured β-Bi2O3-TiO2 nanotube array composite film for photoelectrochemical cathodic protection applications, Corrosion Science https://doi.org/10.1016/j.corsci.2018.02.048.
[15] Chen, D., Wu, S., Fang, J., Lu, S., Zhou, G. Y., Feng, W., Yang, F., Chen, Y., Fang, Z. Q., 2018, A nanosheet-like α-Bi2O3/g-C3N4 heterostructure modified by plasmonic metallic Bi and oxygen vacancies with high photodegradation activity of organic pollutants, Separation and Purification Technology 193 (2018) 232–241.
[16] B. Ohtani, Y. Ogawa, S. Nishimoto, J. Phys. Chem. B 5647 (1997) 3746–3752.
[17] N. Mahdjoub, N. Allen, P. Kelly, V. Vishnyakov, J. Photochem. Photobiol. A: Chem.211 (2010) 59–64.

[18] Peng, F., Ni, Y., Zhou, Q., Kou, J., Lu, C., Xu., Z., New g-C3N4, based photocatalytic cement with enhanced visible-light photolytic activity by constructing muscovite sheet/SnO2 structure, Constructing and Building Materials, Volume 179.10 August 2018, pages 315-325.